Proceedings of The 2021 IEEE International
Conference on Real-time Computing and Robotics
July 15-19, 2021, Xining, China

UCAS-Hand: An Underactuated Powered Hand Exoskeleton for Assisting Grasping Task

Houcheng Li, Long Cheng, Zhengwei Li, Guotao Li

Abstract— **This paper presents a novel underactuated coupled adaptive hand exoskeleton, called UCAS-Hand, which is designed to assist users with weak muscle strength to complete the operation of daily living items. In mechanical design, the proposed UCAS-Hand considers the human-robot kinematic compatibility, grasping adaptability for different objects, portability with motors attached to the hand, force transfer efficiency with applying normal force to the finger phalanges, and passive backdrivability with low gear reduction ratio motor. The UCAS-Hand can realize finger underactuated motions such as flexion/extension and thumb underactuated motions such as flexion/extension, abduction/adduction, and thumb opposability. To minimize the backlashes of bevel gear transmission, a spherical four-bar mechanism and a spherical seven-bar mechanism are designed for the index finger and thumb mechanisms, respectively. Finally, the experiment is implemented to reveal the characteristics of the UCAS-Hand.**

I. INTRODUCTION

With the increasing number and proportion of China's elderly population, China is currently an ageing society [1]. Most elderly people normally lose partial or total ability to operate objects with their hands, which significantly affects their activities of daily living (ADL). At present, passive assistive devices are mainly used to assist the elderly in daily life, such as pen gripper, manual gripping tongs, self-help holders, *etc*. However, these assistive devices can not actively provide grip strength (only passive assistance), have a single function (usually one assistive device can only correspond to one daily operation behaviour, and need to replace assistive devices in to complete other operations), and can not solve the problem of elderly people's hand tremors unconsciously. Therefore, assisting hand operation is regarded as one most critical need for the elderly.

Fortunately, some wearable hand assistive exoskeletons have been developed to assist the elderly with weak muscle strength to enhance their hand grasp function in ADL. Comparing to the hand rehabilitation exoskeletons and hand haptic exoskeletons, there are some special design requirements for hand assistive exoskeletons, which are discussed in [2], [3] deeply. General design requirements are summarized as follows. First, assistive exoskeletons need to have human-robot kinematic compatibility to avoid misalignments between the robot and the user joint during movement, which ensure the user's safety at all times. Second, it is required that assistive exoskeletons have instant adjustability for different tasks and adapt to different objects depending on the contact forces on the phalange. Third, assistive exoskeletons should allow the wearer to move around to manipulate objects rather than sitting or standing in place, which means portability is also important for assistive exoskeletons. In this respect, underactuation may be a beneficial concept to apply. Fourth, assistive exoskeletons must be actively or passively backdrivable to ensure wearers can move their fingers freely rather than restricting users' hand movements. Fifth, the force exerted by the assistive exoskeleton on the finger phalange needs to be vertical, because tangential forces may cause the finger junction to slip and affect the use of the exoskeleton. Moreover, the easy wearability is also of significance to assistive exoskeletons.

In the literature, some state-of-the-art hand assistive exoskeletons have been designed to enhance hand motor function for patients and the elderly. According to the transmission mode, the power-assisted exoskeleton can be divided into three types: linkage-based design, cable-based design, pneumatic-based design. Hand assistive exoskeletons with linkage-based design can generate more stable force and are much easier to maintain and reliable comparing to two other design [4]–[8]. Moreover, it is easier to achieve bidirectional movement of the finger (flexion/extension, abduction/adduction). To reduce weights of wearable parts, increase the portability of overall exoskeleton systems, and realize any shape and size of the grip, underactuation is adopted for the design of the hand assistive exoskeleton. In [4], a linkage-based underactuated hand exoskeleton is developed for grasping power assistance. The remote center of motion (RCM) capability is fully achieved by a purely linkage-type mechanism placed on the lateral side of the finger without considering human-robot kinematic compatibility. This hand structure is more compact and lightweight. However, this mechanism is difficult to guarantee the human-robot axes alignment when using it over a long period of time. Moreover, this hand exoskeleton can only actively drive the index finger movement and lacks the all-important thumb movement in assisting human grasping. In [5], [6], a linkage-based underactuated hand exoskeleton is designed to assist users in performing grasping tasks with consideration of human-robot kinematic compatibility. However, to achieve underactuation and normal force, it looks bulkier and affects its powered assisting task.

This work is supported in part by Beijing Municipal Natural Science Foundation (Grant No. JQ19020) and National Natural Science Foundation of China (Grant Nos. 62025307 and U1913209).

H. Li, L. Cheng, Z. Li, and G. Li are all with the State Key laboratory of Management and Control for Complex Systems, Institute of Automation, Chinese Academy of Sciences, Beijing 100190, China. H. Li and L. Cheng are also with the School of Artificial Intelligence, University of Chinese Academy of Sciences, Beijing 100049, China. {lihoucheng2017, long.cheng, lizhengwei2017, guotao.li}@ia.ac.cn. All correspondences should be addressed to the corresponding author Dr. Long Cheng (long.cheng@ia.ac.cn).

2021 IEEE International Conference on Real-time Computing and Robotics (RCAR) | 978-1-6654-3678-6/21/$31.00 ©2021 IEEE | DOI: 10.1109/RCAR52367.2021.9517383

Hand assistive exoskeletons with cable-based design have some unique advantages, such as lightweight, portable, and compact [9]–[14]. However, there is a loss of tension force because of friction between the cable and sheath. Meanwhile, it is difficult to obtain a precise system model comparing to linkage-based assistive exoskeletons. Moreover, the cable drive also brings hysteresis effect. Therefore, accurate control of the system is a great challenge. In [9], a cable-based power finger-thumb exoskeleton is designed for powered assistance. This hand exoskeleton realizes the human-robot axes alignment by forming a virtual four-bar mechanism, in which the phalanx and joints of the human finger are regarded as a part of the four-bar mechanism. However, the thumb exoskeleton only considers the opposition movement of the carpometacarpal (CMC) joint and lacks the independent movement of adduction/abduction and flexion/extension of the CMC joint. The hand exoskeleton given in [10] is designed based on the concept of self-alignment mechanism with Bowden-cable-based series elastic actuation. This exoskeleton can achieve bidirectional and independent joint torque control to make it safe and comfortable. However, the abduction-adduction motion of the CMC joint adopts the ROM design rather than the self-alignment axis design. Moreover, the large size of the mechanism may limit its applicability as an assistive exoskeleton.

Hand assistive exoskeletons with pneumatic-based design are more lightweight, comfortable, and easier to achieve human-robot kinematic compatibility due to the low elastic modulus of the soft material [15]–[20]. However, the bidirectional force transmission is difficult to achieve because of the cavity structure design. The overall pneumatic system consists of many modules, such as valves, air pumps and flow sensors, which ultimately make the system bulky and heavy and prevent the system from being portable. Moreover, it can assist users in grasping objects only in certain shapes rather than grasping objects with generic shapes. The analysis of the dynamics of the soft exoskeleton is a tough job, which makes the desired control of the soft exoskeleton a challenge.

In this paper, a novel linkage-based underactuated coupled adaptive hand exoskeleton, called UCAS-Hand, is presented. The UCAS-Hand consists of the index finger part and the thumb part, has 5 DoFs (the metacarpophalangeal (MCP) and proximal interphalangeal (PIP) joints of the index finger including 2 DoFs, the carpometacarpal (CMC) and MCP joint of the thumb including 3 DoFs.), is actuated by two motors, and is worn by buckling the Velcro straps. In the mechanical design, the phalanges and joints of the human finger form part of the closed-loop mechanism to realize human-robot kinematic compatibility. The UCAS-Hand adopts the underactuation principle to realize any shape and size of the grip and increase the portability of the overall exoskeleton system. To reduce the influence of tangential shear forces, the slider joint is introduced as the interface between the finger phalanx and the exoskeleton to ensure that only normal forces are applied on the finger phalanges. Moreover, the UCAS-Hand is passively backdrivable by using a motor with a low gear reduction ratio. A spherical four-bar linkage and a spherical seven-bar linkage are applied on the index finger and thumb mechanisms, respectively, to minimize the backlashes caused by the use of bevel gear transmission. Meanwhile, the spherical seven-bar linkage is also used to couple the abduction/adduction and flexion/extension of the thumb CMC joint. Finally, the kinematic model of the UCAS-Hand is analyzed.

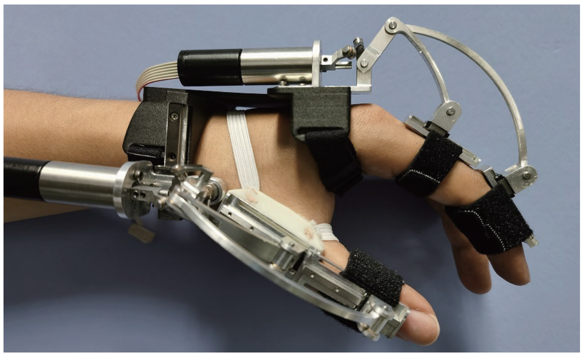

Fig. 1. Overview of the proposed UCAS-Hand mounted on a subject's hand for experimentation.

The main contributions of this paper are the following

1) Compared to the other linkage-based hand exoskeletons, to the best of the authors knowledge, the UCAS-Hand is the first one to achieve the self-alignment axis of the CMC joint (both flexion/extension and abduction/adduction).
2) The UCAS-Hand can realize the self-adaptive grasp to different sizes and shapes of objects, apply only norma forces on the finger phalanges, and is passively backdrivable without restricting the free movement of the hand.
3) The UCAS-Hand realizes the thumb underactuation movement by constructing a spherical seven-bar linkage to ensure the compactness of the whole structure. Meanwhile, the introduction of the spherical mechanism also minimize the backlashes of bevel gear transmission.

This paper is organized as follows. The mechanical design of the UCAS-Hand is introduced in Section II. The kinematic models are developed in Section III. Section IV gives experiments to validate the functional correctness of the proposed UCAS-Hand. Finally, Section V concludes this study and presents the future work plan.

II. Mechanical Design

The overview of the proposed UCAS-Hand is illustrated in Fig. 1. Figure 2 presents the CAD model of the proposed UCAS-Hand worn on a human's left hand. The UCAS-hand consists of the index finger part and the thumb part, both of which are fixed on the dorsal side of the hand. The index finger part of the UCAS-Hand can realize the flexion/extension motion of the MCP and PIP joints (total 2 DoFs) by an index motor, a 4R spherical mechanism and an underactuated mechanism. The thumb finger part of the UCAS-Hand can achieve the flexion/extension motion of the CMC and MP joints and the abduction/adduction motion of the CMC joint (total 3 DoFs) by an thumb motor, a 7R spherical mechanismand an underactuated mechanism. The linkages of

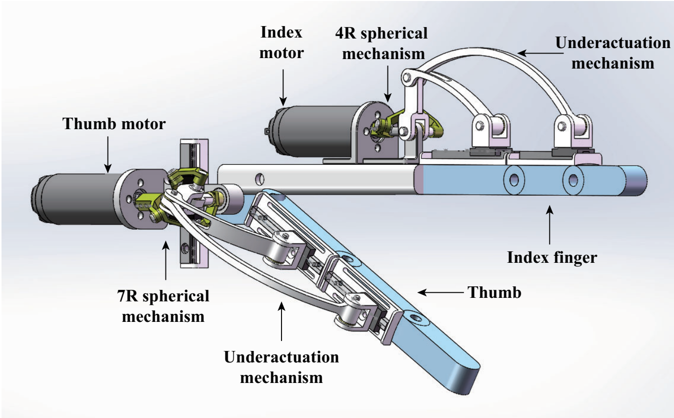

Fig. 2. CAD model of the proposed UCAS-Hand worn on a human's left hand.

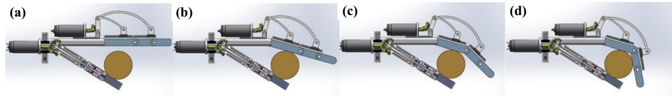

Fig. 3. An animated demonstration of power grasping process of the index finger part of the proposed UCAS-Hand.

the underactuated mechanism are made of Aluminum alloy, and the linkages of the spherical mechanism are made of steel. Based on the functional range of motion of the joints of the hand suggested in [21], the desired flexion/extension motion ranges of the MCP and PIP joints of the index finger are $\theta_M = 0° - 60°, \theta_P = 0° - 60°$, respectively. The desired flexion/extension and abduction/addudction motion ranges of the CMC joint are $\theta_{C1} = 0° - 40°, \theta_{C2} = 0° - 60°$, respectively. The desired flexion/extension motion range of the MP joint are $\theta_{MP} = 0° - 40°$, respectively.

Figure 3 specifically shows how underactuated grasping motion of the index finger part is generated. Before contact occurs on the index finger, the UCAS-Hand actuates the MCP joint of the index finger until the proximal phalange first reaches and touches the grasping object. When the motion of the MCP joint is constrained due to the contact forces on the proximal phalange, the PIP joint continue flexing until the intermediate phalange reaches and touches the grasping object. On contrary, the extension of the index finger starts from the PIP joint and then transfers to the MCP joint until the index finger is fully extended. Because the movements of the DIP and PIP joint are physiologically coupled together, the drive for the DIP joint was omitted in the UCAS-Hand design to reduce the weight of the whole exoskeleton.

The underactuated grasping motion of the thumb part is demonstrated in Fig. 4. At the beginning of the grasping object, the UCAS-Hand actuates the abduction motion of the CMC joint until reaching the physical limits of the mechanism or the user actively restricts the abduction of the CMC joint. The flexion and extension motion of the CMC and MP joints of the thumb is similar to the index finger. The extension of the index finger starts from the MP joint and then transfers to the CMC joint until the thumb comebacks to the initial position. In the mechanical design of the thumb part of the UCAS-Hand, the drive for the IP joint of the thumb was ignored to reduce the complexity of the mechanism.

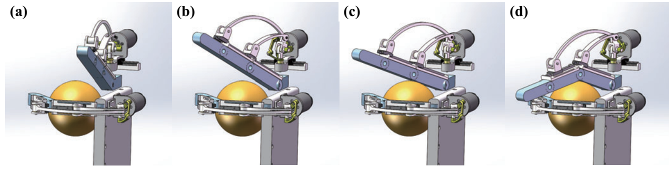

Fig. 4. An animated demonstration of power grasping process of the thumb part of the proposed UCAS-Hand.

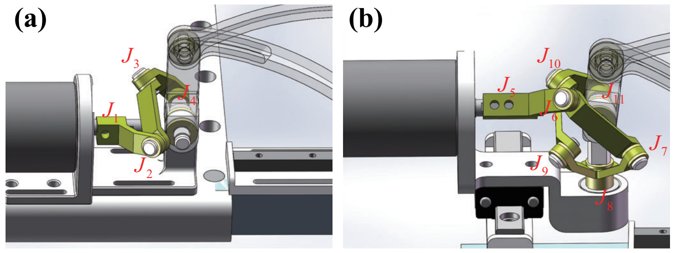

Fig. 5. (a) 4R spherical mechanism for torque transmission in index finger part of the UCAS-Hand, (b) 7R spherical mechanism for torque transmission in thumb part of the UCAS-Hand.

The 4R spherical mechanism is designed to realize torque transmission between the two perpendicular rotation axes (motor axes J_1 and actuating joint J_4) as shown in Fig. 5. Comparing to the bevel gear pair traditionally used in torque commutation, the 4R spherical mechanism can effectively avoid backlashes between two bevel gears. The 7R spherical mechanism is designed to achieve torque transmission between the abduction/adduction movement of the CMC joint and the flexion/extension movement of the CMC joint. This 7R spherical mechanism has one characteristic: the abduction/adduction and flexion/extension movements of the CMC joint one of them can move when the other is restricted. This characteristic is analyzed in Section IV.

III. Kinematic and Statics

A. *Kinematic of the Index Finger Part of the UCAS-Hand*

Figure 6 presents the definition of kinematic parameters of the index finger part of the UCAS-Hand. In the kinematic model, the coordinate frame is located at the point o_1 which is also the revolute joint A associating with the output joint J_4 of the 4R spherical mechanism. The MCP and PIP joints of the index finger are defined as points M and P with the rotations specified as θ_M and θ_P. The kinematic model includes 3 passive revolute joints at points B, C, E with the rotations specified as θ_B, θ_C, θ_E and 2 passive slide joints at points D, F with the translations specified as l_1 and l_2. l_{ij} presents the length between the point i and point j. In the kinematic model, two closed-loop chains contain all unknown parameters, which are presented as follows.

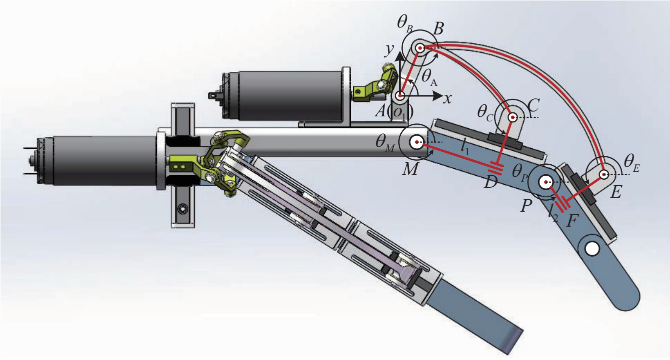

Fig. 6. Kinematic parameters of the index finger part of the UCAS-Hand.

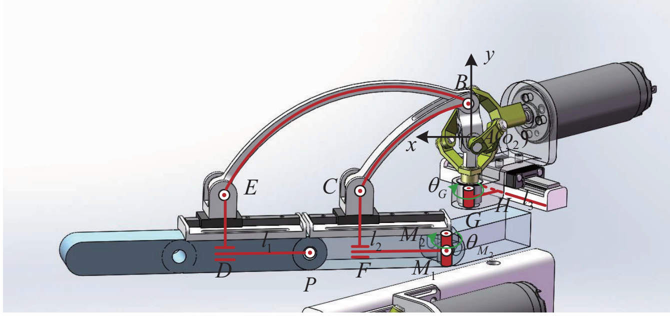

Fig. 7. Kinematic parameters of the thumb finger part of the UCAS-Hand.

The MCP chain is made up of points A, B, C, D, M, which consists of a virtual plane five-bar mechanism. The closed-loop equation of the MCP chain is given by

$$l_{\mathrm{AB}}e^{i\theta_{\mathrm{A}}} + l_{\mathrm{BC}}e^{i\theta_{\mathrm{B}}} + l_{\mathrm{CD}}e^{i\theta_{\mathrm{C}}} = l_{\mathrm{AM}}e^{i\theta_{\mathrm{AM}}} + l_1 e^{i\theta_{\mathrm{M}}}, \quad (1)$$

where θ_{AM} is the vector angle of the $\overrightarrow{AM}$, which is a constant value, and $\theta_{\mathrm{C}} = \theta_{\mathrm{M}} - \frac{\pi}{2}$. The unknown parameters are $\{\theta_{\mathrm{A}}, \theta_{\mathrm{B}}, \theta_{\mathrm{M}}, l_1\}$.

The PIP chain consists of points A, E, F, P, M which forms a virtual plane five-bar mechanism. The closed-loop equation of the PIP chain is presented as follows

$$l_{\mathrm{AE}}e^{i\theta_{\mathrm{AE}}} + l_{\mathrm{EF}}e^{i\theta_{\mathrm{E}}} = l_{\mathrm{AM}}e^{i\theta_{\mathrm{AM}}} + l_{\mathrm{MP}}e^{i\theta_{\mathrm{M}}} + l_2 e^{i\theta_{\mathrm{P}}}, \quad (2)$$

where θ_{AE} is the vector angle of the $\overrightarrow{AE}$, which differs from θ_{A} by a constant value, and $\theta_{\mathrm{E}} = \theta_{\mathrm{P}} - \frac{\pi}{2}$. The unknown parameters are $\{l_2, \theta_{\mathrm{p}}\}$.

The equation (1) and equation (2) contains 4 nonlinear equation. By the given MCP and PIP joint angles $\{\theta_{\mathrm{M}}, \theta_{\mathrm{P}}\}$, the solutions of the unknown parameters $\{\theta_{\mathrm{A}}, \theta_{\mathrm{B}}, l_1, l_2\}$ can be uniquely determined. Actually, the six unknown parameters $\{\theta_{\mathrm{A}}, \theta_{\mathrm{B}}, \theta_{\mathrm{M}}, \theta_{\mathrm{P}}, l_1, l_2\}$ are not independent at the same time, and only four unknown parameters are independent at different stages of the grasping.

B. Kinematic of the Thumb Part of the UCAS-Hand

The definition of kinematic parameters of the index finger part of the UCAS-Hand is shown in Fig. 7. The kinematic model of the flexion/extension movements of the CMC and MP joints is the same as the kinematic model of the index finger part. Regarding the kinematic model of the abduction/adduction movement of the CMC joint, the point M_2 is abstractly represented as the joint of the abduction/adduction of the CMC joint with the rotations specified as θ_{M_2}. The revolute joint G with the rotation specified as θ_G is driven by the 7R spherical mechanism to achieve the abduction/adduction movement of the CMC joint. Point G is a passive slide joint with the translation specified as l_3.

The abduction/adduction kinematic chain consists of the points H, G, F, M_2, and the kinematic model is as follows

$$\begin{cases} \theta_{\mathrm{M}_2} = \theta_{\mathrm{G}}, \\ \Delta l_3 = (\Delta l_2 + x_{\mathrm{M}_2\mathrm{G}}) \cos\theta_{\mathrm{M}_2}, \end{cases} \quad (3)$$

where $\Delta l_2, \Delta l_3$ are the translational values of the slide joint, $x_{\mathrm{M}_2\mathrm{G}}$ represents the vertical distance between the axis of M_2 and the axis of G when joint G does not rotate.

C. Kinematic of the 4R Spherical Mechanism

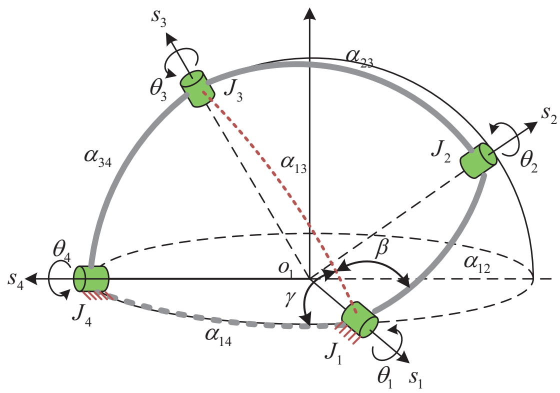

Fig. 8. Kinematic parameters of the 4R spherical mechanism.

Figure 8 shows the definition of kinematic parameters of the 4R spherical mechanism. The revolute joint J_1 is connected to the index DC motor and fixed, and the revolute joint J_4 is fixed on the underactuated mechanism of the index finger part and drives the flexion and extension movements of the MCP and PIP joints. Angle α_{14} is required to be $90°$ so that the motor axis can be vertical to the joint A axis shown in Fig. 6. Angles α_{12}, α_{23}, and α_{34} can be independently chosen. The rotations of links J_1J_2, J_2J_3, J_3J_4 are denoted as $\theta_1, \theta_2, \theta_3$. θ_4 is the spherical angle between the link J_1J_4 and the link J_3J_4. The relationship between θ_1 and θ_4 can be calculated by using spherical trigonometry as follows

$$\begin{cases} \cos\alpha_{23} = \cos\alpha_{13}\cos\alpha_{12} + \sin\alpha_{13}\sin\alpha_{12}\cos\beta, \\ \cos\alpha_{13} = \cos\alpha_{34}\cos\alpha_{14} + \sin\alpha_{34}\sin\alpha_{14}\cos\theta_4, \\ \cos\theta_1 = \cos(\pi - \beta - \gamma), \\ \dfrac{\sin\gamma}{\sin\alpha_{34}} = \dfrac{\sin\theta_4}{\sin\alpha_{13}}, \\ \sin\alpha_{13}\cos\gamma = \cos\alpha_{34}\sin\alpha_{14} - \sin\alpha_{34}\cos\alpha_{14}\cos\theta_4. \end{cases} \quad (4)$$

By simplifying the equation set (4), the length α_{23} can be expressed as follows

$$\cos\alpha_{23} = \cos\alpha_{12}\cos\alpha_{34}\cos\alpha_{14} + \sin\alpha_{14}\sin\alpha_{34}\cos\alpha_{12}\cos\theta_4$$

$$
\begin{aligned}
& - \sin\alpha_{14}\cos\alpha_{34}\sin\alpha_{12}\cos\theta_1 \\
& + \sin\alpha_{34}\sin\alpha_{12}\sin\theta_1\sin\theta_4 \\
& + \sin\alpha_{34}\sin\alpha_{12}\cos\theta_1\cos\theta_4\cos\alpha_{14}.
\end{aligned} \tag{5}
$$

Equation 5 shows the implicit relationship between the angle θ_1 and the angle θ_4. A correspondent explicit expression of the angle θ_4 as function of the parameters $\alpha_{12}, \alpha_{23}, \alpha_{34}, \alpha_{14}$, and θ_1 can be obtained as follows

$$
\theta_4 = 2\arctan\left(\frac{X_1 \pm (X_1^2 + X_2^2 - X_3^2)^{\frac{1}{2}}}{X_2 - X_3}\right) \tag{6}
$$

where

$$
\begin{aligned}
X_1 =& \sin\alpha_{34}\sin\alpha_{12}\sin\theta_1, \\
X_2 =& \sin\alpha_{14}\sin\alpha_{34}\cos\alpha_{12} + \sin\alpha_{34}\sin\alpha_{12}\cos\theta_1\cos\alpha_{14}, \\
X_3 =& \cos\alpha_{12}\cos\alpha_{34}\cos\alpha_{14} - \sin\alpha_{14}\cos\alpha_{34}\sin\alpha_{12}\cos\theta_1 \\
& - \cos\alpha_{23}.
\end{aligned}
$$

D. Kinematic of the 7R Spherical Mechanism

The definition of the kinematic parameters of the 7R spherical mechanism is illustrated in Fig. 9. The revolute joint J_5 is connected to the thumb DC motor and fixed. The revolute joint J_8 is fixed on the revolute joint G presented in Fig. 7 and drive the abduction/adduction movements of the CMC joint. The revolute joint J_{11} is fixed on the joint A in underactuated mechanism of the thumb part shown in Fig. 7 and drives the flexion/extension movements of the CMC and MP joints. Angle α_{58} is required to be $90°$ so that the motor axis can be vertical to the joint G axis shown in Fig. 7. Angle α_{8-11} is required to be $90°$ so that the joint A axis can be vertical to the joint G axis shown in Fig. 7. Angle α_{79} is required to be a constant value. Angles α_{56}-α_{10-11} can be independently chosen. The rotations of links $J_5J_6, J_6J_7 - J_{10}J_{11}$ are denoted as $\theta_5, \theta_6 - \theta_{10}$. θ_{11} is the spherical angle between the link $J_{10}J_{11}$ and the link J_8J_{11}.

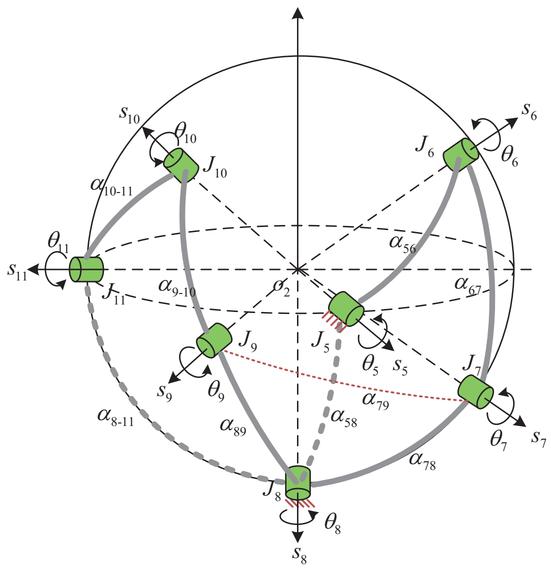

Fig. 9. Kinematic parameters of the 7R spherical mechanism

When the flexion/extension movement of the CMC joint is constricted by the user or reaching the physical limits of the mechanism, it means the joint J_{11} is not rotated. At this point, the thumb motor only drives the adduction and abduction motion of the thumb CMC joint, and the abduction/adduction angle corresponds to joint θ_8. The joints J_5, J_6, J_7 and J_8 forms a spherical mechanism. The chain of $J_5J_6J_7J_8$ can be viewed as a whole, and rotates around J_8. The explicit relationship between the angle θ_5 and the angle θ_8 can be expressed as follows

$$
\theta_8 = 2\arctan\left(\frac{Y_1 \pm (Y_1^2 + Y_2^2 - Y_3^2)^{\frac{1}{2}}}{Y_2 - Y_3}\right) \tag{7}
$$

where

$$
\begin{aligned}
Y_1 =& \sin\alpha_{78}\sin\alpha_{56}\sin\theta_5, \\
Y_2 =& \sin\alpha_{58}\sin\alpha_{78}\cos\alpha_{56} + \sin\alpha_{78}\sin\alpha_{56}\cos\theta_5\cos\alpha_{58}, \\
Y_3 =& \cos\alpha_{56}\cos\alpha_{78}\cos\alpha_{58} - \sin\alpha_{58}\cos\alpha_{78}\sin\alpha_{56}\cos\theta_5 \\
& - \cos\alpha_{67}.
\end{aligned}
$$

When the abduction/adduction movement of the CMC joint is constricted by the user or reaching the physical limits of the mechanism, it means the joint J_{11} is rotated. At this point, the motor torque is transferred from J_5 to J_8 and then to J_{11} through two 4R spherical mechanisms. The explicit relationship between the angle θ_5 and the angle θ_{11} can be obtained as follows

$$
\theta_{11} = 2\arctan\left(\frac{Z_1 \pm (Z_1^2 + Z_2^2 - Z_3^2)^{\frac{1}{2}}}{Z_2 - Z_3}\right) \tag{8}
$$

where

$$
\begin{aligned}
Z_1 =& \sin\alpha_{10-11}\sin\alpha_{89}\sin\theta_8, \\
Z_2 =& \sin\alpha_{8-11}\sin\alpha_{10-11}\cos\alpha_{89} \\
& + \sin\alpha_{10-11}\sin\alpha_{89}\cos\theta_8\cos\alpha_{8-11}, \\
Z_3 =& \cos\alpha_{89}\cos\alpha_{10-11}\cos\alpha_{8-11} \\
& - \sin\alpha_{8-11}\cos\alpha_{10-11}\sin\alpha_{89}\cos\theta_8 - \cos\alpha_{9-10}, \\
\theta_8 =& 2\arctan\left(\frac{Y_1 \pm (Y_1^2 + Y_2^2 - Y_3^2)^{\frac{1}{2}}}{Y_2 - Y_3}\right).
\end{aligned}
$$

Based on above kinematic analysis, the proposed 7R spherical mechanism has one characteristic: the abduction/adduction and flexion/extension movements of the CMC joint one of them can move when the other is restricted. This mechanical design is conducive to realizing the seamless switch between the two movements of abduction/adduction and flexion/extension of the CMC joint.

IV. EXPERIMENTAL RESULTS AND DISCUSSIONS

To verify the functional correctness of the proposed UCAS-Hand, the proposed UCAS-Hand was tested by a healthy subject. In the experiment, the subject wore the UCAS-Hand and completes a series of grasping tasks, such as prismatic grasp, circular grasp, medium wrap, and tip pinch. Figure 10 presents the subject can complete different grasping tasks with the help of the UCAS-Hand without any prior knowledge on the objects. In the grasping tasks, the UCAS-Hand can adapt to objects with different shapes and sizes, which was consistent with the mechanical analysis.

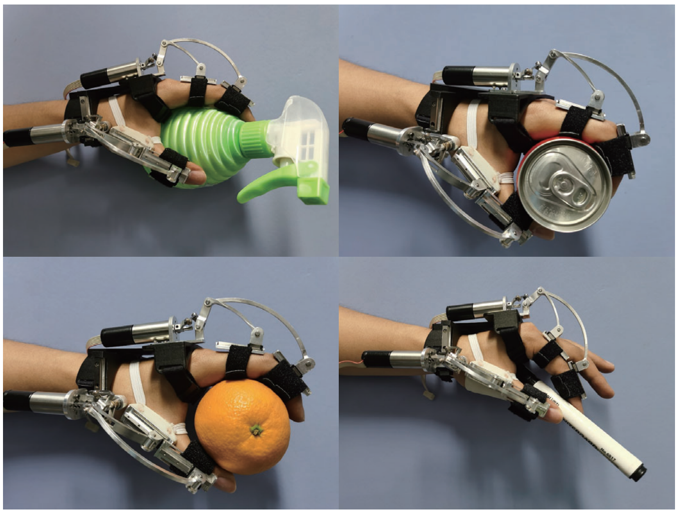

Fig. 10. The four grasp types, prismatic grasp, circular grasp, medium wrap, and tip pinch, can be executed with the UCAS-Hand.

V. CONCLUSIONS AND FUTURE WORK

This paper presents UCAS-Hand, a novel linkage-based underactuated coupled adaptive hand exoskeleton, to give power assistance. The UCAS-Hand achieves the human-robot kinematic compatibility design for all actuated joints. To the best of the authors knowledge, the UCAS-Hand is the first one to realize the self-alignment axis of the CMC joint (both flexion/extension and abduction/adduction) with under-actuation. The UCAS-Hand possesses the grasping adaptability for different objects with generic shapes, portability, high force transfer efficiency, and passive backdrivability. A spherical 4R mechanism and a spherical 7R mechanism are designed on the index finger and thumb mechanisms, respectively, to reduce the backlashes and transmit torque.

The current work mainly focuses on the mechanical design of the UCAS-Hand. There is still a lot of work to be done in the future. First, the position control of the UCAS-Hand is needed to be completed. Second, the compliant control need to be implemented in the UCAS-Hand to realize actively backdrivability and guarantee the stability of the human-robot interaction [22], [23]. Third, more experiments are needed to verify the usability of the UCAS-Hand.

REFERENCES

[1] United Nations, Department of Economic and Social Affairs, Population Division (2019). *2019 Revision of the World Population Prospects* (ST/ESA/SER.A/423).

[2] M. Sarac, M. Solazzi, and A. Frisoli, "Design requirements of generic hand exoskeletons and survey of hand exoskeletons for rehabilitation, assistive, or haptic use," *IEEE Transactions on Haptics*, vol. 12, no. 4, pp. 400-413, 2019.

[3] Q.A. Boser, M.R. Dawson, J.S. Schofield, G. Dziwenko, and J.S. Hebert, "Defining the design requirements for an assistive powered hand exoskeleton," *bioRxiv*, DOI: 10.1101/492124, 2018.

[4] M.B. Hong, S.J. Kim, Y.S. Ihn, G.C. Jeong, and K. Kim, "KULEX-Hand: An underactuated wearable hand for grasping power assistance," *IEEE Transactions on Robotics*, vol. 35, no. 2, pp. 420-432, 2019.

[5] M. Gabardi, M. Solazzi, D. Leonardis, and A. Frisoli, "Design and evaluation of a novel 5 DoF underactuated thumb-exoskeleton," *IEEE Robotics and Automation Letters*, vol. 3, no. 3, pp. 2322-2329, 2018.

[6] M. Sarac, M. Solazzi, E. Sotgiu, M. Bergamasco, and A. Frisoli, "Design and kinematic optimization of a novel underactuated robotic hand exoskeleton," *Meccanica*, vol.52, pp. 749-761, 2017.

[7] F. Wang, M. Shastri, C. L. Jones, V. Gupta, C. Osswald, X. Kang, D.G. Kamper, and N. Sarkar, "Design and control of an actuated thumb exoskeleton for hand rehabilitation following stroke," in *Proceedings of IEEE International Conference on Robotics and Automation*, Shanghai, China, May 2011, pp. 3688-3693.

[8] D. Marconi, A. Baldoni, Z. McKinney, M. Cempini, S. Crea, and Nicola Vitiello, "A novel hand exoskeleton with series elastic actuation for modulated torque transfer," *Mechatronics*, vol. 61, pp. 69-82, 2019.

[9] M. Cempini, M. Cortese, and N. Vitiello, "A powered finger-thumb wearable hand exoskeleton with self-aligning joint axes," *IEEE/ASME Transactions on Mechatronics*, vol. 20, no. 2, pp. 705–716, 2015.

[10] P. Agarwal,Y. Yun, J. Fox, K. Madden, and A.D. Deshpande, "Design, control, and testing of a thumb exoskeleton with series elastic actuation," *The International Journal of Robotics Research*, vol. 36, no. 2, pp. 355–375, 2017.

[11] L. Cheng, M. Chen and Z. Li, "Design and control of a wearable hand rehabilitation robot," *IEEE Access*, vol. 6, pp. 74039-74050, 2018.

[12] H. Li, L. Cheng, and Z. Li,"Design and control of an index finger exoskeleton with cable-driven translational joints," in *Proceedings of International Conference on Advanced Robotics and Mechatronics*, Shenzhen, China, Dec. 2020, pp. 540-545.

[13] T. Bützer, O. Lambercy, J. Arata, and R. Gassert1, "Fully wearable actuated soft exoskeleton for grasping assistance in everyday activities," *Soft Robotics*, DOI: 10.1089/soro.2019.0135, 2020.

[14] N. Sun, G. Li, and L. Cheng,"Design and validation of a self-aligning index finger exoskeleton for post-stroke rehabilitation," submitted to *IEEE Transactions on Neural Systems and Rehabilitation Engineering* for possible publication, 2021.

[15] K.H.L. Heung, R.K.Y. Tong, A.T.H. Lau, and Z. Li, "Robotic glove with soft-elastic composite actuators for assisting activities of daily living," *Soft Robotics*, DOI: 10.1089/soro.2017.0125, 2019.

[16] B.B. Kang, H. Choi, H. Lee, and K.J. Cho, "Exo-glove poly II: A polymer-based soft wearable robot for the hand with a tendon-driven actuation system," *Soft Robotics*, vol.6, no.2, pp. 214-227, 2019.

[17] H. Li, L. Cheng, Z. Li, and W. Xue, "Active disturbance rejection control for a fluid-driven hand rehabilitation device," *IEEE/ASME Transactions on Mechatronics*, vol. 26, no. 2, pp. 841–853, 2021.

[18] Z. Li, L. Cheng, and Q. Song, "An ultra-stretchable and highly sensitive photoelectric effect-based strain sensor: implementation and applications," *IEEE Sensors Journal*, vol. 21, no. 4, pp. 4365-4376, 2020.

[19] M. Feng, D. Yang, and G. Gu, "High-force fabric-based pneumatic actuators with asymmetric chambers and interference-reinforced structure for soft wearable assistive gloves," *IEEE Robotics and Automation Letters*, vol. 6, no. 2, pp.3105-3111, 2021.

[20] N. Takahashi, S. Furuya, and H. Koike, "Soft exoskeleton glove with human anatomical architecture: Production of dexterous finger movements and skillful piano performance," *IEEE Transactions on Haptics*, vol. 13, no. 4, pp. 679-690, 2020.

[21] M.C. Hume, H. Gellman, H. McKellop, and R.H. Brumfield Jr, "Functional range of motion of the joints of the hand," *The Journal of Hand Surgery*, vol. 15, no. 2, pp. 240-243, 1990.

[22] L. Cheng, W. Liu, C. Zhou, Y. Zou, and Z. Hou, "Automated silicon-substrate ultra-microtome for automating the collection of brain sections in array tomography," *IEEE/CAA Journal of Automatica Sinica*, vol. 8, no. 2, pp. 389-401, 2021.

[23] R. Cao, L. Cheng, C. Yang, and Z. Dong, "Iterative assist-as-needed control with interaction factor for rehabilitation robots," *Science China Technological Sciences*, vol. 64, no. 4, pp. 836-846, 2021.